

# We are IntechOpen, the world's leading publisher of Open Access books Built by scientists, for scientists

6,900

Open access books available

185,000

International authors and editors

200M

Downloads

Our authors are among the

154

Countries delivered to

TOP 1%

most cited scientists

12.2%

Contributors from top 500 universities



WEB OF SCIENCE™

Selection of our books indexed in the Book Citation Index  
in Web of Science™ Core Collection (BKCI)

Interested in publishing with us?  
Contact [book.department@intechopen.com](mailto:book.department@intechopen.com)

Numbers displayed above are based on latest data collected.  
For more information visit [www.intechopen.com](http://www.intechopen.com)



# A Description of the Transport Critical Current Behavior of Polycrystalline Superconductors Under the Applied Magnetic Field

C.A.C. Passos, M. S. Bolzan, M.T.D. Orlando, H. Belich Jr,  
J.L. Passamai Jr., J. A. Ferreira and E. V. L. de Mello

Additional information is available at the end of the chapter

<http://dx.doi.org/10.5772/50429>

## 1. Introduction

Since their discovery in 1986 the high- $T_c$  superconductors (HTSC) have been employed in several applications. The expectation with the discover of new devices sparked the beginning of an intense research to understand the parameters which control the physical properties of these materials. With the goal to the practical applications, the critical current density ( $J_c$ ) is one of the crucial parameters that must be optimized for HTSC [1]. Thus the aim of this chapter is to describe the transport critical current behavior of polycrystalline superconductors under the applied magnetic field.

According to Gabovich and Mosieev [2], there is a dependence of the superconducting properties on the macrostructure of ceramic. They studied the  $\text{BaPb}_{1-x}\text{Bi}_x\text{O}_3$  metal oxide superconductor properties which are a consequence of the granularity of the ceramic macrostructure and the existence of weak Josephson links between the grains. In this case, the superconductivity depends strongly on the presence of grain boundaries and on the properties of the electronic states at the grain boundaries. This determines the kinetic characteristics of the material. For instance, the temperature dependence of the electrical conductivity of oxide superconductor is related to complex Josephson medium.

Nowadays it is well known that the  $J_c$  in polycrystalline superconductors is determined by two factors: the first is related to the defects within the grains (intragrain regions) such as point defects, dislocations, stacking faults, cracks, film thickness, and others [3, 4]. When polycrystalline samples are submitted to magnetic field, the intragranular critical current can be limited by the thermally activated flux flow at high magnetic fields. Secondly the critical current depends on the grain connectivity, that is, intergrain regions. Rosenblatt *et*

*al.* [5] developed an idea to discuss the key concept of granularity and its implications for localization in the normal state and para coherence in the superconducting state. For arrays formed by niobium grains imbedded in epoxy resin [6] the coherent penetration depth or screening current are influenced by the intergrain regions. In fact, the main obstacles to intergranular critical current flow are weak superconductivity regions between the grains [7], called weak links (WLs) [8]. Ceramic superconductor samples present a random network for the supercurrent path, with the critical current being limited by the weakest links in each path. This Josephson-type mechanism of conduction is responsible to the dependence of the critical current density on the magnetic field  $J_c(H)$ , as noted in several experimental studies [9–11]. On the other hand, the intragranular critical current is limited by an activated flux flow at high temperature and a high magnetic field [9, 12, 13].

Considering these factors, Altshuler *et al.* [14] and Muller and Matthews [15] introduced the possibility of calculating the  $J_c(H)$  characteristic under any magnetic history following the proposal of Peterson and Ekin [16]. Basically the model considers that the transport properties of the junctions are determined by an "effective field" resulting from superposition of an external applied field and the field associated with magnetization of the superconducting grains.

Another theoretical approach to the  $J_c(H)$  dependence in a junction took into account the effect of the magnetic field within the grains. This study has revealed that the usual Fraunhofer-like expression for  $J_c(H)$  [17, 18] should be written as  $J_c(H) \propto \sin(bH^{1/2})/(bH^{1/2})$ , which we call the modified Fraunhofer-like expression [19]. Mezzetti *et al.* [20] and González *et al.* [21] also proposed models to describe  $J_c(H)$  behavior taking into account the latter expression. In both studies the authors concluded that a Gamma-type WL distribution controls the transport critical current density.

González *et al.* considered two different regimes [21]: for low applied magnetic field, a linear decrease in  $J_c$  with the field was observed, whereas for high fields  $J_c(H) \propto (1/B)^{0.5}$  dependence was found. Here we have decided to follow the same approach and extend the analytical results to all applied magnetic fields.

Usually polycrystalline ceramics samples contain grains of several sizes and the junction length changes from grain to grain. In addition, the granular samples may exhibit electrical, magnetic or other properties which are distinct from those of the material into the grains [5]. The average  $J_c(H)$  is obtained by integrating  $J_c(H)$  for each junction and taking into account a distribution of junction lengths in the sample. It was demonstrated that the WL width follows a Gamma-type distribution [22]. This function yields positive unilateral values and is always used to represent positive physical quantities. Furthermore, this Gamma distribution is the classical distribution used to describe the microstructure of granular samples [23] and satisfactorily reproduces the grain radius distribution in high- $T_c$  ceramic superconductors [24].

## 2. Basic properties

A superconductor exhibits two interesting properties: the first one is the electrical resistance of the material abruptly drops to zero at critical temperature  $T_c$ . The superconductor is

able to carry electrical current without resistance. This phenomenon is related to the perfect diamagnetism. The second feature of superconductivity is also known as Meissner effect. In this case a superconductor expels an external applied magnetic field into its interior.

This struggle between superconductivity and magnetic field penetration select two important behaviors. If a superconductor does not permit any applied magnetic flux, it is known as Type I superconductor. In this case, if the superconducting state is put in the presence of a too high magnetic field, the superconductivity is destroyed when the magnetic field magnitude exceeds the critical value  $H_c$ . Other superconductor category is the Type II material in which the magnetic properties are more complex. For this material the superconductor switches from the Meissner state to a state of partial magnetic flux penetration. The penetration of magnetic flux starts at a lower field  $H_{c1}$  to reach at an upper a higher field  $H_{c2}$ .

In addition to the two limiting parameters  $T_c$  and  $H_c$ , the superconductivity is also broken down when the material carries an electrical current density that exceeds the critical current density  $J_c$ . In the Ginzburg-Landau theory, the superconducting critical current density can be written as

$$J_c = \left(\frac{2}{3}\right)^{2/3} \frac{H_c}{\lambda}. \quad (1)$$

The current density given by Eq. (1) is sometimes called the *Ginzburg-Landau depairing current density*.

Once into the superconductor state, it is possible to cross the superconductor surface changing only the current. In this case, even for  $T < T_c$  and  $H < H_c$  with the material reaching its normal state, and with loss of its superconductor properties.

### 3. Josephson-type mechanism

Following the discovery of the electron tunneling (barrier penetration) in semiconductor, Giaever [25] showed that electron can tunnel between two superconductors. Subsequently, Josephson predicted that the Cooper pairs should be able to tunnel through the insulator from one superconductor to the other even zero voltage difference such the supercurrent is given by [26]

$$J = J_c \sin(\theta_1 - \theta_2) \quad (2)$$

where  $J_c$  is the maximum current in which the junction can support, and  $\theta_i$  ( $i = 1, 2$ ) is the phase of wave function in  $i$ th superconductor at the tunnel junctions. This effect takes in account dc current flux in absence of applied electric and magnetic fields, called as the *dc Josephson effect*.

If a constant nonzero voltage  $V$  is maintained across the Josephson junction (barrier or weak link), an ac supercurrent will flow through the barrier produced by the single electrons tunneling. The frequency of the ac supercurrent is  $\nu = 2eV/\hbar$ . The oscillating current of Cooper pairs is known as the *ac Josephson effect*. These Josephson effects play a special role in superconducting applications.

It was mentioned that the behavior of a superconductor is sensitive to a magnetic field, so that the Josephson junction is also dependent. Therefore another mode of pair tunneling is a

tunneling current with an oscillatory dependence on the applied magnetic flux  $\sin(\pi\Phi/\Phi_0)$ , where  $\Phi_0$  is the quantum of magnetic flux. This phenomenon is known as *macroscopic quantum interference effect*.

### 3.1. Basic equations of Josephson effect

As mentioned, the Josephson effect can occur between two superconductors weakly connected. Some types of linkage are possible such as sketched in Figure (1). These configurations depends on the application types in which the weak link can be:

1. an insulating, corresponding to a SIS junction, in which case the insulate layer can be in order of 10 - 20 Å;
2. a normal metal, corresponding to a SNS junction of typical dimensions 102 - 104 Å;
3. a very fine superconducting point presses on a flat superconductor;
4. a narrow constriction (microbridge) of typical dimensions like the coherence length 1 μm.

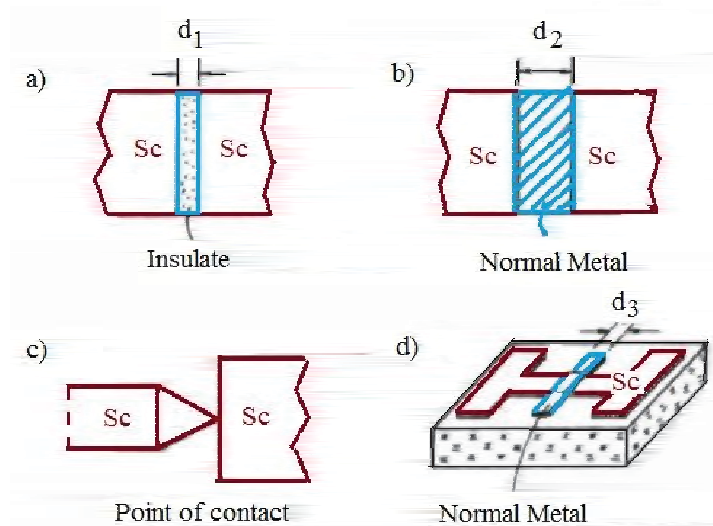


**Figure 1.** Four types of Josephson junctions: (a) SIS with  $d_1 = 10 - 20$  Å, (b) SNS where  $d_2 = 102 - 104$  Å, (c) Point of contact, and (d) microbridge with  $d_3 \approx 1\mu\text{m}$  [27].

Consider that two superconductors are separated from each other by an insulating layer. The junction is of thickness  $d$  normal to the  $y$ -axis with cross-sectional dimensions  $a$  and  $c$  along  $x$  and  $z$ , respectively. A voltage is applied between the superconductors and the junction is thick enough so that one assumes the potential to be zero in the middle of the barrier. Figure (2) displays Josephson junctions corresponding to a SIS junction.

In Feynman approach  $\Psi_1$  and  $\Psi_2$  are the quantum mechanical wavefunction of the superconducting state in the left and the right superconductor, respectively. This system is determined by coupled time-dependent Schroedinger equations:

$$\begin{aligned} i\hbar \frac{\partial \Psi_1}{\partial t} &= -2eV_1 \Psi_1 + K \Psi_2 \\ i\hbar \frac{\partial \Psi_2}{\partial t} &= -2eV_2 \Psi_2 + K \Psi_1, \end{aligned} \quad (3)$$



The behavior of  $J_c$  can also be analyzed the Ambegaokar and Baratoff theory [29]. Ambegaokar and Baratoff generalized the Josephson tunnel theory and derived the tunnelling supercurrent on the basis of the BCS theory for a s-wave homogeneous superconductor. In this approach, the temperature dependence of critical current is given with the following expression:

$$J_c = \frac{\pi}{2eR_N S} \Delta(T) \tanh\left[\frac{\Delta(T)}{2k_B T}\right] \quad (6)$$

when  $T$  near  $T_c$ ,  $\Delta(T) \simeq 1.74\Delta_0(1 - T/T_c)^{1/2}$  is the superconducting gap parameter from the BCS theory.  $R_N$  is the normal-state resistance of the junction,  $S$  is the cross section of a junction, and  $e$  and  $k_B$  are electron charge and Boltzmann constant, respectively. For temperature relatively close to  $T_c$ , we can suppose the condition  $\Delta(T) \ll k_B T$  and the  $\tanh[\Delta(T)/2k_B T] \approx \Delta(T)/2k_B T$ . Taking this into account, Eq. (8) is transformed into [21]

$$J_c \approx \frac{\pi}{4eR_N S} \Delta_0^2 \left[1 - \frac{T}{T_c}\right]. \quad (7)$$

And in limiting  $T \rightarrow 0$ ,

$$J_c \approx \frac{\pi}{4eR_N S} \frac{\Delta_0}{e}. \quad (8)$$

To calculate the Josephson coupling energy for cuprate superconductors that have a d-wave order parameter with nodes, we recall the work of Bruder and co-workers [30]. They have found that the tunneling current behaves in a similar fashion of s-wave superconductors junction and the leading behavior is determined by tunneling from a gap node in one side of a junction into the effective gap in the other side. Consequently, as a first approximation to the Josephson coupling energy  $E_J$ , we describe the theory of s-wave granular superconductors [29] to an average order parameter  $\Delta$  in the grains.

In 1974, Rosenblatt [31] also analysed the tunnelling supercurrent through Josephson barriers, but in bulk granular superconductors (BGS). He proposed that the superconducting order parameter of an assembly of superconducting grains in the absence of applied current can be represented by a set of vectors in the complex plane  $\Delta_\alpha = |\Delta| \exp(i\phi_\alpha)$ , where  $\phi_\alpha$  is the superconducting phase in  $\alpha$ th grain. He showed the arrays of Josephson junctions become superconducting in two stages. At the bulk transition temperature  $T_o$ , the magnitude of the order parameter of each grain becomes nonzero [32]. He considered two neighboring grains along an axis with complex superconducting order parameters  $\Delta_1$  and  $\Delta_2$ . Therefore, the Josephson junction can be modelled by [33]

$$H_t = - \sum_{\langle ij \rangle} J_{ij} S_i^+ S_j^- \quad (9)$$

where  $H_t$  is pair tunnelling Hamilton,  $S_{ij}^\pm$  is destruction and creation operators,

$$J_{ij} = \frac{R_c}{2R_{ij}} \Delta(T) \tanh\left[\frac{\Delta(T)}{2k_B T}\right], \quad (10)$$

the Josephson coupling energy between grains  $i$  and  $j$ ,  $R_c = \pi\hbar/2e^2$  and  $R_{ij}$  is normal state resistance of the junctions between grains  $i$  and  $j$ .



Until now it was discussed Josephson junctions independent of magnetic field. However the Josephson contacts exhibit macroscopy quantum effects under magnetic field. In order to examine the effect of applying a magnetic field into the junctions, considering the Josephson junctions as sketched in Figure (3) with a magnetic field  $B_0 \vec{k}$  applied along the vertical  $z$  direction,

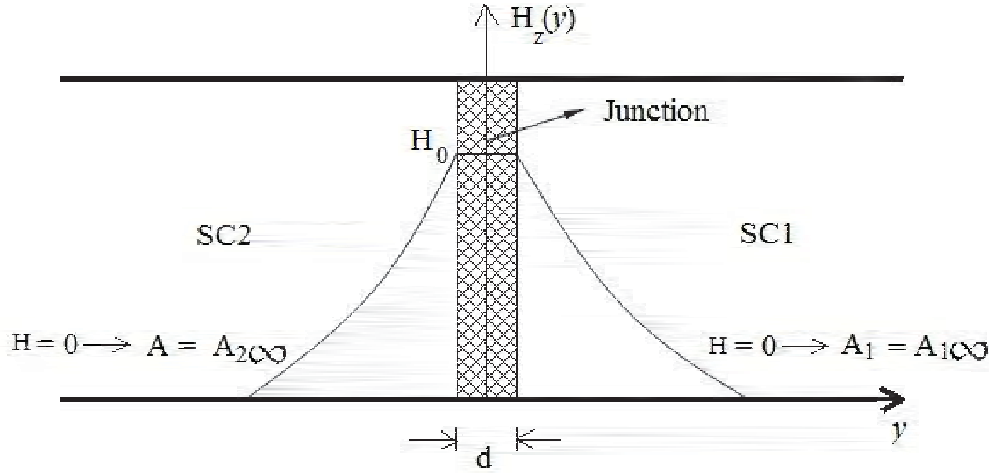


**Figure 3.** Behavior of the magnetic field in a Josephson junction.  $A_1$  is potential in the superconductor 1 and  $A_2$  is potential in the superconductor 2 [28].

It is assumed because of symmetry, the magnetic field  $H(y)$  has no  $x$ - or  $z$ -direction dependence, but it varies in  $y$ -direction insofar the field penetrates into superconductor.

$$\vec{H} = H_z(y) \vec{k}.$$

It is known that magnetic field is derived from potential vector  $\vec{H} = \nabla \times \vec{A}$ , such that

$$\vec{A} = A_x(y) \vec{i}$$

with  $|y| = \frac{d}{2}$ . Inside the barrier the material is not superconducting and  $H_z = H_0$ . Now it must choose an integration contour as shown in Figure (4)

Consider the equation that relates the gradient of the phase of the wave function of the superconducting state with the magnetic vector potential integration of a closed path where the current is zero.

$$\oint \vec{\nabla} \Theta(r) d\vec{l} = \frac{2\pi}{\Phi_0} \oint \vec{A} \cdot d\vec{l}. \quad (11)$$

For the integration path ABCD

$$\int_A^B \vec{\nabla} \Theta(r) d\vec{l} + \int_B^C \vec{\nabla} \Theta(r) d\vec{l} + \int_C^D \vec{\nabla} \Theta(r) d\vec{l} = \frac{2\pi}{\Phi_0} \left( \int_A^B \vec{A} \cdot d\vec{l} + \int_B^C \vec{A} \cdot d\vec{l} + \int_C^D \vec{A} \cdot d\vec{l} \right). \quad (12)$$

The integrals in AB and CD are zero due to orthogonality of the vectors  $\vec{A} \cdot d\vec{l}$ .

$$\Theta_1 - \Theta_{10} = \frac{2\pi}{\Phi_0} A_{1\infty} (x - x_0). \quad (13)$$



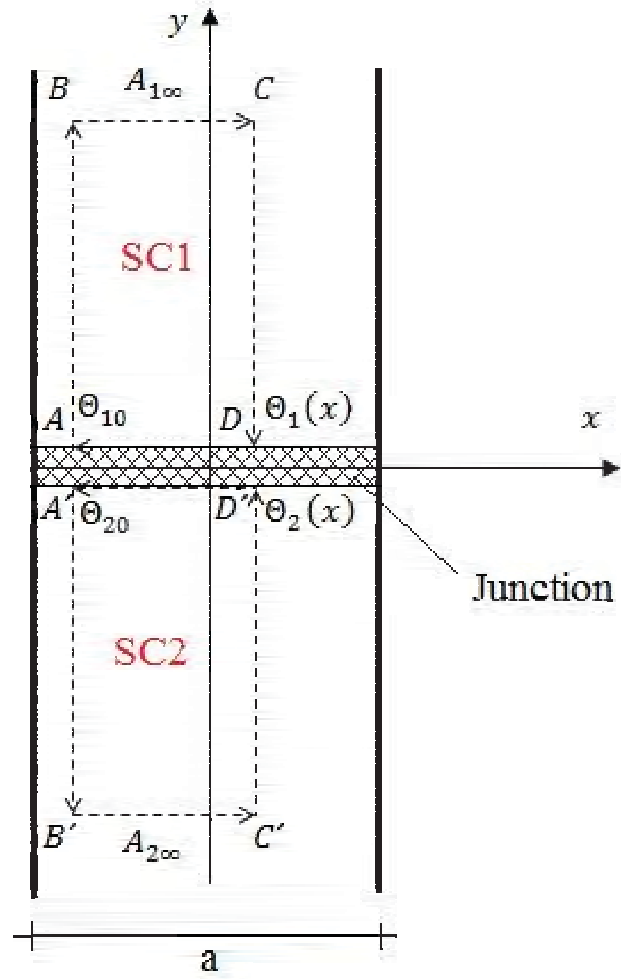


**Figure 4.** Path of integration around the Josephson junction. One superconductor SC1 is to the above of the insulating barrier and the other superconductor SC2. It was considered a weak-link tunnel short junction. [28]

To  $\Theta_2(x)$  the integration result is similar, but it must be to consider the  $A'B'C'D'$  path

$$\Theta_2 - \Theta_{20} = -\frac{2\pi}{\Phi_0} A_{2\infty}(x - x_0). \quad (14)$$

Since the aim is to obtain the phase difference  $\delta(x)$ ,

$$\delta(x) = \Theta_2(x) - \Theta_1(x) = \delta_0 + \frac{2\pi}{\Phi_0}(A_{1\infty} + A_{2\infty})x, \quad (15)$$

where  $\delta_0 = \Theta_{20} - \Theta_{10}$  is phase difference at  $x_0$ . The total magnetic flux is given by

$$\Phi = \int \vec{A} \cdot d\vec{l} = \int \vec{H} \cdot dS\vec{n},$$

and then

$$\Phi = a(A_{1\infty} + A_{2\infty}).$$

Thus the phase difference is given by

$$\delta(x) = \delta_0 + \frac{2\pi\Phi}{\Phi_0} \left( \frac{x}{a} \right). \quad (16)$$

Inserting equation (16) into equation (8) yields after integration over area  $S = ac$  cross section of the barrier, the tunneling current is

$$I = J_c \int \sin(\delta_0) dx dz = c J_c \int_{-a/2}^{+a/2} \sin\left(\delta_0 + \frac{2\pi\Phi}{\Phi_0} x\right) dx. \quad (17)$$

Taking  $u = \delta_0 + \frac{2\pi\Phi}{\Phi_0}$ , the tunneling current becomes

$$I = ac J_c \frac{\Phi_0}{\pi\Phi} \sin(\delta_0) \sin\left(\frac{\pi\Phi}{\Phi_0}\right) \quad (18)$$

When is this current maximum? The answer is for phase difference  $\delta_0 = \frac{\pi}{2}$ . Hence,

$$I_{max} = I_c \left| \frac{\sin(\pi\Phi/\Phi_0)}{(\pi\Phi/\Phi_0)} \right|, \quad (19)$$

where  $I_c = ac J_c$  is the critical current. This is named the *Josephson junction diffraction equation* and shows a Fraunhofer-like dependence of the magnetic field as is displayed in Figure (5)

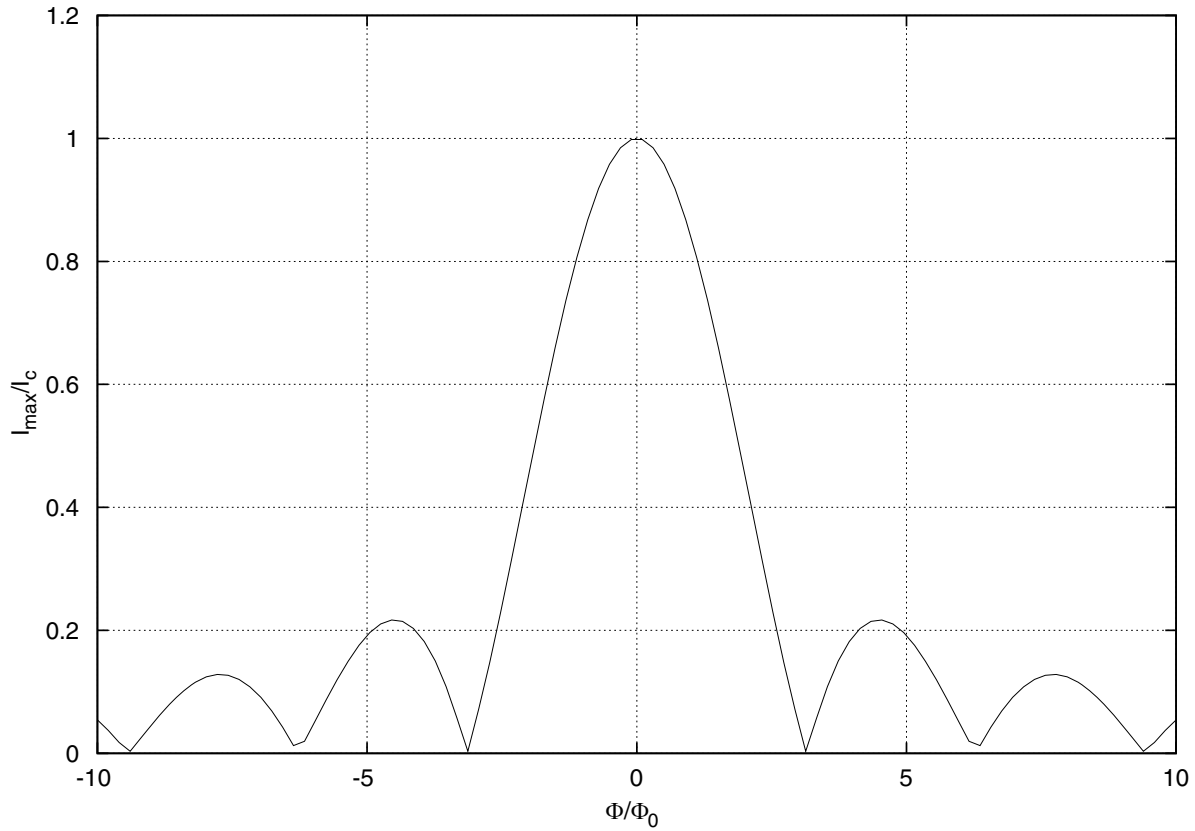


**Figure 5.** Josephson Fraunhofer diffraction pattern dependence of magnetic field [34].

#### 4. Critical current model

It is well known which ceramic superconductor samples present a random network for the supercurrent path, with the critical current being limited by the weakest links in each path. Moreover, magneto-optical studies have demonstrated that the magnetic field first penetrates grains associated with these regions, even for very low values of  $H$ . Consequently, it would be interesting to estimate the influence of the magnetic field on the overall  $J_c$  of a sample taking into account the previous remarks. There are some general hypotheses about transport properties in polycrystalline ceramic superconductors on application of a magnetic field. (i) The electric current percolates through the material and heating begins to occur in WLs and in channels between them. This means that the critical current measured in the laboratory is an intergranular current. (ii) The junction widths among grains are less than the Josephson length, and the magnetic field penetrates uniformly into the junctions. (iii) The sample temperature during transport measurement must be close to the critical temperature. Under these conditions, the junction widths are less than the bulk coherence length and the Cooper-pairs current is given by Josephson tunneling. (iv) Near the critical temperature the magnetic field first penetrates WLs and, at practically the same time, the grains.

Normally polycrystalline ceramics samples contain grains of several sizes and the junction length changes from grain to grain. The average  $J_c(H)$  is obtained by integrating  $J_c(H)$  for each junction and taking into account a distribution of junction lengths in the sample. This function yields positive unilateral values and is always used to represent positive physical quantities. Furthermore, this Gamma distribution is the classical distribution used to describe the microstructure of granular samples [23] and reproduces the grain radius distribution in high- $T_c$  ceramic superconductors [24].

Following the previous discussion, we can describe  $J_c(H)$  as a statistical average of the critical current density through a grain boundary. In the same way as Mezzetti *et al.* [20] and González *et al.* [21], we consider that the weak-link width fits a Gamma-type distribution [35]. For a magnetic field higher or lower than the first critical field, the usual Fraunhofer diffraction pattern or the modified pattern is used to describe  $J_c(H)$  for each grain boundary. Thus,

$$J_c(H) = J_{c0} \int_{-\infty}^{+\infty} P(u) \left| \frac{\sin(\pi u/u_0)}{\pi u/u_0} \right| du \quad (20)$$

$$P(u) = \begin{cases} \frac{u^{m-1} e^{(-u/\eta)}}{\eta^m \Gamma(m)} & u \geq 0 \\ 0 & u < 0, \end{cases}$$

where  $\Gamma(m)$  is the Gamma function which is widely tabulated [22, 36]:

$$\Gamma(m) = \int_0^{\infty} w^{m-1} e^{-w} dw$$

when  $m$  is a real number. Or  $\Gamma(m) = (m-1)!$  if  $m$  is a positive integer. The parameters  $m$  and  $\eta$ , both positive integer, determine the distribution form and scale (width and height), respectively [21]. The variable  $u$  represents the WL length. The quantity  $u_0$  is defined as  $u_0 = \phi_0/\Lambda_0 H$ , where  $\phi_0$  is the quantum flux and  $\Lambda_0$  is the effective thickness of the WL.

Following the same González *et al.* [21] procedure, we have:

$$J_c(\alpha) = J_{c0} \frac{\alpha^m (-1)^m}{(m-1)!} \frac{\partial^{m-2}}{\partial \alpha^{m-2}} \left[ \frac{\coth(\alpha/2)}{\alpha^2 + \pi^2} \right], \quad (21)$$

where the variable  $\alpha$  is defined as  $\alpha = u_0/\eta = \phi_0/(\eta\Lambda_0 H)$ . To obtain a simpler expression for the transport critical current density, we develop Eq. (21) in the ranges  $0 < \alpha < \pi/2$  and  $\alpha \geq \pi/2$  [37].

#### 4.1. Expression for $J_c(H)$ for $0 < \alpha < \pi/2$

The function  $F(z) = [\coth(z/2)] = (z^2 + \pi^2)$  has singular points at  $z = \pm i\pi$ , but is analytical at all remaining points on the disc  $|z| = \pi$ . Thus, we expanded  $F(z)$  for the disc  $|z| < \pi$ .

The hyperbolic cotangent has the expansion [36]

$$z \coth(z/2) = 2 \left[ \sum_{n=0}^{\infty} \frac{b_{2n}}{2n!} z^{2n} \right] \quad |z| < \pi, \quad (22)$$

where  $b_{2n}$  are the Bernoulli numbers ( $b_0 = 1, b_2 = 1/6, b_4 = -1/30, b_6 = 1/42, \dots$ ) given by [36]:

$$b_{2n} = [(-1)^{n-1} 2(2n)!] / [(2\pi)^{2n}] \zeta(2n),$$

where  $\zeta(2n)$  is the Zeta Riemann function. The function  $[1/(z^2 + \pi^2)]$  is represented by the Taylor series around zero:

$$\frac{1}{z^2 + \pi^2} = \frac{1}{\pi^2} \sum_{j=0}^{\infty} (-1)^j \frac{z^{2j}}{\pi^{2j}}. \quad (23)$$

Now we can compute the Cauchy product of the series (22) and (23) to obtain:

$$\frac{z \coth(z/2)}{z^2 + \pi^2} = \frac{2}{\pi^2} \left[ 1 + \sum_{n=1}^{\infty} \left( \sum_{j=0}^{\infty} \frac{(-1)^{n+j} b_{2j}}{\pi^{2n-2j} (2j)!} \right) z^{2n} \right]. \quad (24)$$

It is convenient to define

$$\beta_n = \left[ \sum_{j=0}^{\infty} \frac{(-1)^{n+j} b_{2j}}{\pi^{2n-2j} (2j)!} \right] = \frac{2}{\pi^{2n}} \left[ \sum_{j=0}^{\infty} \frac{(-1)^{n-1}}{(2)^{2j}} \zeta(2j) \right]. \quad (25)$$

Thus, we can rewrite Eq. (24) as:

$$\frac{z \coth(z/2)}{z^2 + \pi^2} = \frac{2}{\pi^2} \left[ \frac{1}{z} + \sum_{n=1}^{\infty} \beta_n z^{2n-1} \right] \quad z \neq 0. \quad (26)$$

The critical current density  $J_c(\alpha)$  is calculated by taking  $z = \alpha$  in Eq. (26) and differentiating it  $(m-2)$  times, term by term. This yields:

$$J_c(\alpha) = \frac{2J_{c0}}{\pi^2(m-1)} \alpha \left[ 1 + (-1)^m \sum_{n_0}^{\infty} \binom{2n-1}{m-2} \beta_n \alpha^{2n} \right] \quad (0 < \alpha < \pi/2), \quad (27)$$

where  $n_0$  is the lower integer and  $n_0 \geq (m-1)/2$ . This expression (27) for  $J_c$  is valid for the range  $0 < \alpha < \pi$ . However, for more efficient calculation, we suggest that it is only used for the range  $0 < \alpha < \pi/2$ .

Finally, we can express  $J_c$  as a function of  $H$  by substituting the definition of  $\alpha$ ,  $\alpha = u_0/\eta = \phi_0/(\eta\Lambda_0 H)$  in Eq. (27). Thus [37],

$$J_c(H) = \frac{2J_{c0}}{\pi^2(m-1)} 1.02 \sqrt{\frac{H_0^*}{H}} \left[ 1 + (-1)^m \sum_{n_0}^{\infty} (1.02)^{2n} (m)^{2n} \binom{2n-1}{m-2} \beta_n \left( \frac{H_0^*}{H} \right)^{2n} \right], \quad (28)$$

where  $H_0^* = \phi_0(\langle m\eta \rangle \Lambda_0) = \phi_0/\bar{u}\Lambda_0 = \phi_0/A$  is the effective magnetic field characteristic for each polycrystalline superconductor, and  $A$  is the area perpendicular to the magnetic field direction. It is important to emphasize that the first term of Eq. (28) was determined by González *et al.* [21] for high magnetic fields ( $\alpha \ll 1$ ).

The estimate errors for the series in Eq. (28) were calculated as [37]:

$$E_N = \frac{5\pi^2}{12} \left[ \frac{4}{3} \binom{2N-1}{m-2} + \left( 1 + \frac{(-1)^m}{3^{m-1}} \right) \right] (1/2)^{2N}, \quad (29)$$

where  $E_N$  is defined as the  $N$ -order error of the series in Eq. (28).

#### 4.2. Expression for $J_c(H)$ for $\alpha \geq \pi/2$

The hyperbolic cotangent in Eq. (21) can also be written as:

$$\coth(z/2) = 1 + \left( \frac{2e^{-z}}{1 - e^{-z}} \right) = 1 + 2 \sum_{k=1}^{\infty} e^{-kz} \quad (\text{Re } z > 0), \quad (30)$$

since the series in (30) is a Dirichlet type and is convergent at all semi-planes  $\text{Re } z > 0$ . Dividing Eq. (30) by  $(z^2 + \pi^2)$ , we obtain:

$$\frac{\coth(z/2)}{z^2 + \pi^2} = \frac{1}{z^2 + \pi^2} + \frac{2}{z^2 + \pi^2} \sum_{k=1}^{\infty} e^{-kz} \quad (\text{Re } z > 0). \quad (31)$$

The expression for the critical current density for  $\alpha \geq \pi/2$  is obtained by differentiation of Eq. (31) in Eq. (21)  $(m-2)$  times. Thus,

$$J_c(z) = \frac{J_{c0} z^m (-1)^m}{(m-1)!} \left[ D^{m-2} \left( \frac{1}{z^2 + \pi^2} \right) + D^{m-2} \left( \frac{2}{z^2 + \pi^2} \sum_{k=1}^{\infty} e^{-kz} \right) \right],$$

$$J_c(z) = \frac{J_{c0} z^m (-1)^m}{(m-1)!} \left[ f_{m-2}(z) + R(z) \right], \quad (32)$$

where

$$f_{m-2}(z) = D^{m-2} \left( 1/(z^2 + \pi^2) \right)$$

and

$$R(z) = D^{m-2} \left[ 2/(z^2 + \pi^2) \sum_{k=1}^{\infty} e^{-kz} \right].$$

For  $z = \alpha$

$$R(\alpha) = 2 \sum_{k=1}^{\infty} \left[ \sum_{p=0}^{m-2} (-1)^{m-p} \binom{m-2}{p} \times f_p(\alpha) k^{m-p-2} \right] e^{-k\alpha} \quad (33)$$

and  $f_p(\alpha)$  can be written as

$$f_p(p) = \frac{(-1)^p p!}{(\alpha^2 + \pi^2)^{p+1}} \left[ \frac{(p+1)!}{p!} \alpha^p - \frac{(p+1)!}{(p-2)!3!} \pi^2 \alpha^{p-2} + \frac{(p+1)!}{(p-4)!5!} \pi^4 \alpha^{p-4} - \dots \right], \quad (34)$$

where  $p$  is greater than or equal to zero. It is advantageous to write  $f_p(\alpha)$  in this form because it is finite for all  $\alpha > 0$ . To obtain a expression for  $J_c(H)$  from Eq. (33), we express  $f_p(\alpha)$  and  $R(\alpha)$  as a function of  $H$ . Thus,

$$f_p(H) = \frac{(-1)^p p!}{m^{2p+2} \left[ \left( \frac{H_0^*}{H} \right)^2 + \frac{\pi^2}{m^2} \right]^{p+1}} \left[ a_{p0} \left( \frac{H_0^*}{H} \right)^p - a_{p1} \left( \frac{H_0^*}{H} \right)^{p-2} + a_{p2} \left( \frac{H_0^*}{H} \right)^{p-4} - \dots \right], \quad (35)$$

where  $a_{p0} = \frac{(p+1)!}{p!} m^p$ ,  $a_{p1} = \frac{(p+1)!}{(p-2)!3!} \pi^2 m^{p-2}$ ,  $a_{p2} = \frac{(p+1)!}{(p-4)!5!} \pi^4 m^{p-4}$ , and so on. It is worth commenting again that  $f_p(H)$  is finite for all values of  $H$  and is defined for  $p > 0$ .  $R(H)$  is written as

$$R(H) = 2 \sum_{k=1}^{\infty} \left[ \sum_{p=0}^{m-2} (-1)^{m-p} \binom{m-2}{p} \times f_p(H) k^{m-p-2} \right] e^{-km \left( \frac{H_0^*}{H} \right)}. \quad (36)$$

Now Eq. (16) can be expressed as [37]:

$$J_c(H) = \frac{J_{c0}(1)^m}{(m-1)!} \left( \frac{H_0^*}{H} \right)^m \left[ f_{m-2}H + R(H) \right]. \quad (37)$$

The series error estimated in  $R(\alpha)$  [Eq. (34)] is [37]:

$$E_{K+1}(\alpha) \leq \frac{e(m-2)!}{\pi} \left[ \sum_{p=0}^{m-2} \frac{1}{(\alpha^2 + \pi^2)^{(m-p-2)/2}} \times \sum_{l=0}^p \frac{K^{p-l}}{(p-l)! \alpha^{l+1}} \right] e^{-k\alpha}, \quad (38)$$

where  $E_{K+1}$  is defined as the  $K+1$ -order error of the series in Eq. (34).

A low applied magnetic field implies that  $\alpha \gg 1$ , and Eq. (37) is transformed to:

$$J_c(H) \approx J_c(0) \left( 1 - \frac{\pi^2(m+1)}{6m} \frac{H}{H_0^*} \right), \quad (39)$$

where  $H_0^* = \frac{\phi_0}{\langle \eta m \rangle^2} = \frac{\phi_0}{\bar{u}^2}$  is a characteristic field that determines the behavior of  $J_c(H)$  in this region. In addition,  $\bar{u}$  represents the mean of the width distribution function  $P(u)$  involved in the transport of Cooper pairs through the sample. Eq. (39) reproduces the quasi-linear behavior that was also reported by Gonzalez *et al.* [21].

## 5. Critical current measurement

Typical  $J_c$  measurements are performed using the four-probe technique with automatic control of the sample temperature, the applied magnetic field and the bias current [14]. Details of the technique and the experimental setup are in Ref. [14] and of the synthesis and sample characterization were published elsewhere [13].

Figure (6) shows the experimental results of [38] for the critical current as a function of the applied field, together with the theoretical expression derived above for the critical field  $H_0^*$  in the figure and for  $m = 2$  and 3. A very close fit to the experimental data is evident for  $m = 2$  for many different applied magnetic fields.

Theoretical models of the magnetic field dependence of the transport critical current density for a polycrystalline ceramic superconductor have been studied at last years [37, 39–41]. Here we have described a tunneling critical current between grains follows a Fraunhofer diffraction pattern or a modified pattern. It is important to emphasize that we followed the same approach as in [21] and extended the analytical results to all applied magnetic fields. A characteristic field ( $H^*$ ) was identified and different regimes were considered, leading to analytical expressions for  $J_c(H)$ : (i) analysis for low applied magnetic fields ( $\alpha \gg 1$ ) revealed quasi-linear behavior for  $J_c(H)$  vs.  $H^*$ ; (ii) for high applied magnetic fields ( $\alpha \ll 1$ ),  $J_c(H)$  is proportional to  $H^{-0.5}$ , as reported in [21].





- [8] Polyanskii, A., Feldmann, D.M., Patnaik, S., Jiang, J., Cai, X., Larbalestier, D., DeMoranville, K., Yu, D., Parrella, R. (2001). Examination of current limiting mechanisms in monocoire Bi<sub>2</sub>Sr<sub>2</sub>Ca<sub>2</sub>Cu<sub>3</sub>O<sub>x</sub> tape with high critical current density, *IEEE Trans. Appl. Supercond.*, Vol. 11 (No. 1) 3269–3272.
- [9] Ben Azzouz, F., Zouaoui, M., Mellekh, A., Annabi, M., Van Tendeloo, G., Ben Salem, M. (2007). Flux pinning by Al-based nanoparticles embedded in YBCO: A transmission electron microscopic study, *Physica C*, Vol. 455 (No. 1-2) 19–24.
- [10] Ekin, J. W., Braginski, A. I., Panson, A. J., Janocko, M. A., Capone, D. W., Zaluzec, N. J., Flandermeyer, B., de Lima, O. F., Hong, M., Kwo, J., Liou, S. H. (1987). Evidence for weak link and anisotropy limitations on the transport critical current in bulk polycrystalline Y<sub>1</sub>Ba<sub>2</sub>Cu<sub>3</sub>O<sub>x</sub>, *J. Appl. Phys*, Vol. 62 (No. 12) 4821–4828.
- [11] Dupart, J. M. , Rosenblatt, J. and Baixeras J. (1977). Supercurrents and dynamic resistivities in periodic arrays of superconducting-normal contacts. *Phys. Rev. B*, Vol. 16 (No. 11), 4815–4825.
- [12] Matsumoto, Y., Higuchi, K., Nishida, A., Akune, T., Sakamoto, N. (2004). Temperature dependence of critical current density and flux creep of Hg(Re)-1223 powdered specimens, *Physica C*, Vol. 412 435–439.
- [13] Passos, C.A.C., Orlando, M.T.D., Fernandes, A.A.R., Oliveira, F.D.C., Simonetti, D.S.L., Fardin, J.F., Belich Jr. H., Ferreira Jr. M.M. (2005). Effects of oxygen content on the pinning energy and critical current in the granular (Hg, Re)-1223 superconductors, *Physica C*, Vol. 419 (No 1-2) 25–31.
- [14] Altshuler, E., Cobas, R., Batista-Leyva, A. J., Noda, C., Flores, L. E., Martínez, C., Orlando, M. T. D. (1999). Relaxation of the transport critical current in high-T<sub>c</sub> polycrystals, *Phys. Rev. B*, Vol. 60 (No. 5) 3673–3679.
- [15] Muller, K.H. and Matthews, D.N. (1993). A model for the hysteretic critical current density in polycrystalline high-temperature superconductors, *Physica C* Vol. 206 (No. 3-4) 275–284.
- [16] Peterson, R.L. and Ekin, J.W. (1988). Josephson-junction model of critical current in granular Y<sub>1</sub>Ba<sub>2</sub>Cu<sub>3</sub>O<sub>7-d</sub> superconductors, *Phys. Rev. B*, Vol. 37 (No. 16) 9848–9851.
- [17] Bulaevskii L. N. , Clem J. R., Glazman L. I. (1992). Fraunhofer oscillations in a multilayer system with Josephson coupling of layers. *Phys. Rev. B*, Vol. 46 (No. 1), 350–355.
- [18] Fistul, M.V. and Giuliani, G.F. (1993). Theory of finite-size effects and vortex penetration in small Josephson junctions, *Phys. Rev. B*, Vol. 51 (No. 2) 1090–1095.
- [19] Ares, O., Hart, C., Acosta, M. (1995). Transition from magnetic Fraunhofer-like to interferometric behavior in YBCO bridges with decreasing width, *Physica C*, Vol. 242 (No. 1-2) 191–196.
- [20] Mezzetti, E., Gerbaldo, R., Ghigo, G., Gozzelino, L., Minetti, B., Camerlingo, C., Monaco, A., Cuttone, G., Rovelli, A. (1999). Control of the critical current density in YBa<sub>2</sub>Cu<sub>3</sub>O<sub>7-d</sub> films by means of intergrain and intragrain correlated defects, *Phys. Rev. B*, Vol. 60 (No. 10) 7623–7630.
- [21] Gonzalez, J. L., Mello, E.V.L., Orlando, M.T.D., Yague, E.S., Baggio-Saitovitch, E. (2001). Transport critical current in granular samples under high magnetic fields, *Physica C*, Vol. 364–365 347–349.

- [22] Degroot, M.H. (1986). *Probability and Statistics*, Addison-Wesley Pub. Co., ISBN: 020111366X, 9780201113662. Michigan.
- [23] Passos, C. A. C., Orlando, M. T. D., Oliveira, F. D. C., da Cruz, P. C. M., Passamai Jr., J. L., Orlando, C. G. P., Elói, N. A., Correa, H. P. S., Martinez, L. G. (2002). Effects of oxygen content on the properties of the  $\text{Hg}_{0.82}\text{Re}_{0.18}\text{Ba}_2\text{Ca}_2\text{Cu}_3\text{O}_{8+d}$  superconductor, *Supercond. Sci. Technol.*, Vol. 15 (No. 8) 1177–1183.
- [24] Oliveira, F.D.C., Passos, C.A.C., Fardin, J.F., Simonetti, D.S.L., Passamai, J.L., Belich Jr., H., de Medeiros, E.F., Orlando, M.T.D., Ferreira, M.M. (2006). The influence of oxygen partial pressure on growth of the (Hg,Re)-1223 intergrain junction, *IEEE Trans. Appl. Supercond.*, Vol. 16 (No. 1) 15–20.
- [25] Giaever, I. (1960) Eletron tunneling between 2 superconductors, *Physical Review Letters*, Vol. 5 (No.10) 464–466.
- [26] Josephson, B. D. (1962) Possible new effects in superconductive tunnelling, *Physics Letters* Vol. 1 (No.7) 251–25.
- [27] Mourachkine, A. (2004). *Room-Temperature Superconductivity*, Cambridge International Science, ISBN 1-904602-27-4. Cambridge.
- [28] Poole, C. P. , Farach, H. A., Creswick, R. J., Prozorov R. (2007). *Superconductivity*, 2nd. Ed, Acadmemic Press Elsevier, ISBN: 978-0-12-088761-3. Amsterdam.
- [29] Ambegaokar V., and Baratoff, A. (1963). Tunneling between superconductors. *Physical Review Letters* Vol. 10 486.
- [30] Bruder, C., Vanotterlo A., Zimanyi G. T. (1995). Tunnel-junctions of unconventional superconductors. *Phys. Rev. B*, Vol. 51 (No. 18), 12904–12907.
- [31] Rosenblatt, J. (1974). Coherent and paracoherent states in josephson-coupled granular superconductors. *Revue de Physique Appliquée*, Vol. 9 (No. 1), 217–222.
- [32] Simkin, M. V. (1991) Josephson-oscillator spectrum and the reentrant phase transition in granular superconductors. *Phys. Rev. B*, Vol. 44 (No. 13), 7074–7077.
- [33] Lebeau C., Raboutou, A., Peyral, P., and Rosenblatt, J. (1988). Fractal description of ferromagnetic glasses and random Josephon networks. *Physica B*, Vol. 152 (No. 1), 100–104.
- [34] Matsushita, T. (2007). *Flux Pinnig in Superconductors*, Springer, ISBN-10 3-540-44514-5. New York.
- [35] Spiegel, M.R. (1999). *Shcaum's Outline of Theory and Problems of Probability and Statistics*, McGraw-Hill Professional, ISBN: 0070602816, 9780070602816. New York.
- [36] Abramowitz M., Stegun, I.A. (Eds.) (1972), *Handbook of Mathematical Functions with Formulas, Graphs and Mathematical Tables*, 9th printing, Dover, New York.
- [37] Virgens, M. G.: MSc (Thesis in Portuguese). Physics Department, UFES (2002).
- [38] Batista-Leyva, A. J., Cobas, R., Estévez-Rams, E., Orlando, M. T. D., Noda, C., Altshuler, E. (2000). Hysteresis of the critical current density in YBCO, HBCCO and BSCCO superconducting polycrystals: a comparative study, *Physica C*, Vol. 331 (No. 1) 57-66.
- [39] Bogolyubov, N. A. (2010). Pattern of the induced magnetic field in high-temperature superconducting ceramics. *Physica C*, Vol. 470 (No.7-8) 361-364.
- [40] Eisterer, M., Zehetmayer, M., and Weber, H.W. (2003). Current Percolation and Anisotropy in Polycrystalline  $\text{MgB}_2$ . *Physics Review Letters* Vol. 90 (No. 24), 247002-1–247002-4.

- [41] Preseter, M. (1996). Dynamical exponents for the current-induced percolation transition in high- $T_c$  superconductors. *Phys. Rev. B*, Vol. 54 (No. 1), 606–618.